NMR Studies of the Conformations and Location of Nucleotides Bound to the *Escherichia coli* MutT Enzyme[†]

David N. Frick,[‡] David J. Weber,[§,||] Chitrananda Abeygunawardana,[§] Apostolos G. Gittis,[⊥] Maurice J. Bessman,[‡] and Albert S. Mildvan*[,§]

Department of Biology, The Johns Hopkins University, Charles and 34th Streets, Baltimore, Maryland 21218, and Departments of Biological Chemistry and Biophysics and Biophysical Chemistry, The Johns Hopkins School of Medicine, 725 North Wolfe Street, Baltimore, Maryland 21205

ABSTRACT: The MutT enzyme catalyzes the hydrolysis of nucleoside triphosphates to nucleoside monophosphates and pyrophosphate by substitution at the rarely attacked β-phosphorus. Nucleotides containing bulky substituents at the 8 position of the purine ring are preferentially hydrolyzed. The conformation of the MutT-bound nonhydrolyzable substrate analog Mg^{2+}-AMPCPP, determined by 10 intramolecular NOEs and molecular dynamics refinement using a full relaxation matrix analysis with back-calculation of the NOESY intensities, is high *anti* ($\chi = 53 \pm 9°$), with a C2'-*exo*, O1'-*endo* sugar pucker. Similarly, the product of dGTP hydrolysis, dGMP, also binds MutT in a high *anti* ($\chi = 73 \pm 9°$) C1'-*endo* conformation based on seven intramolecular NOEs. Such high *anti* rotations of the base would allow MutT to accommodate nucleotides substituted at the C-8 position with no intramolecular clashes. Changes in chemical shifts in the $^1H-^{15}N$ spectra of the enzyme induced by Mg^{2+} and Mg^{2+}AMPCPP suggest that the metal activator and nucleotide interact with residues in loop I, at the carboxyl end of helix I, loop II, loop III, and β-strands A and B of the secondary structure of MutT. The displacement of Mg^{2+} by Mn^{2+} causes the selective disappearance due to paramagnetic broadening of $^1H-^{15}N$ cross peaks from G37, G38, and K39 in loop I and E57 in helix I. Eleven intermolecular NOEs between Mg^{2+}AMPCPP and hydrophobic residues of MutT are found, three of which are tentatively assigned to L67 in loop II and three to L54 in helix I. Similarly, seven intermolecular NOEs between dGMP and hydrophobic residues of the enzyme are found, four of which are tentatively assigned to L54 and two to V58, both in helix I. These interactions indicate that the loop I−helix I−loop II motif contributes significantly to the active site of MutT in accord with mutagenesis studies and with sequence homologies among MutT-like NTP pyrophosphohydrolases.

The *Escherichia coli mutT* gene codes for the antimutator protein, MutT, which specifically prevents AT-CG transversions and, thereby, decreases the mutation rate in *E. coli* by several orders of magnitude (Treffers *et al.*, 1954; Yanofsky *et al.*, 1966; Fowler *et al.*, 1992). The MutT protein contains a nucleoside triphosphate pyrophosphohydrolase (Bhatnagar *et al.*, 1991), active on all eight canonical nucleoside triphosphates (NTPs)[1] with preference for dGTP (Bhatnagar & Bessman, 1988). Higher activity was found with purine nucleotides containing a bulky substituent at the

8-position (Bhatnagar *et al.*, 1991) which can assume a *syn* conformation in DNA (Tavale & Sobell, 1970). Topal and Fresco (1976) have postulated that guanine, in the *syn* conformation, could mispair with adenine, which would lead directly to the AT → CG transversion found in MutT deficient organisms. The role of the MutT enzyme could well be the removal of mutagenic forms of guanine nucleotides from the deoxynucleoside triphosphate pool (Bhatnagar *et al.*, 1991). Maki and Sekiguchi (1992) have proposed that 8-oxo-dGTP which can mispair with template adenine during DNA synthesis *in vitro* (Cheng *et al.*, 1991) is the substrate of the MutT enzyme.

These considerations suggest that the active site of the MutT enzyme might bind nucleotides in an unusual conformation. The conformation of substrates on MutT is also of interest because MutT catalyzes nucleophilic substitution at the rarely attacked β-phosphorus of an NTP (Weber *et al.*, 1992). The six other enzymes that catalyze such a reaction are complex synthetases. The simple hydrolysis catalyzed by MutT presents a unique opportunity to study the mechanism of enzymatic attack at this electron-dense position (Mildvan, 1979).

The location of nucleotide binding is particularly noteworthy because the MutT family of proteins contains a unique signature sequence conserved throughout nature

---

* To whom correspondence should be addressed. Phone: 410-955-2038. Fax: 410-955-5759.

[‡] Department of Biology, The Johns Hopkins University.

[§] Department of Biological Chemistry, The Johns Hopkins School of Medicine.

[||] Present address: Department of Biological Chemistry, University of Maryland School of Medicine, 108 N. Greene Street, Baltimore, MD 21201.

[⊥] Department of Biophysics and Biophysical Chemistry, The Johns Hopkins School of Medicine.

[⊛] Abstract published in *Advance ACS Abstracts*, April 1, 1995.

[1] Abbreviations: AMPCPP, α,β-methyleneadenosine triphosphate; HSQC, heteronuclear single quantum coherence; NMR, nuclear magnetic resonance; NOE, nuclear Overhauser effect; NOESY, nuclear Overhauser effect spectroscopy; NTP, nucleoside triphosphate; pH*, pH meter reading in ^2H_2O uncorrected for isotope effects; RMSD, root mean square deviation; Tris-Cl, tris(hydroxymethyl)aminomethane hydrochloride; 2D, two-dimensional.

differing from homologies found among other nucleotide binding proteins (Koonin, 1993; Mejean *et al.*, 1994). Amino acid substitutions in this region of MutT dramatically affect protein stability, solubility, and activity (Frick *et al.*, 1994a; Mejean *et al.*, 1994), and proteins containing this conserved sequence have been shown to possess nucleotide pyrophosphohydrolase activity (Bhatnagar & Bessman, 1988; Sakumi *et al.*, 1993; Bullions *et al.*, 1994). The solution secondary structure of MutT has been determined by heteronuclear multidimensional NMR (Abeygunawardana *et al.*, 1993; Weber *et al.*, 1993) and the homologous region has been found to consist of a loop—helix—loop motif which may contribute to a novel nucleotide binding and nucleotide pyrophosphohydrolase site.

In this report, the conformations and environments of the nonhydrolyzable substrate analog Mg^{2+}-AMPCPP and of the product dGMP when bound to MutT are determined from a series of 2D NOESY experiments. Both nucleotides bind in a high *anti* conformation consistent with the substrate preference of MutT for purine nucleotides with bulky substituents at C-8. Upon binding to MutT, Mg^{2+} ions and Mg^{2+}-AMPCPP effect the chemical shifts of backbone ^{15}N and NH resonances of MutT in the conserved loop—helix—loop region. Distance-dependent paramagnetic effects of Mn^{2+} and intermolecular NOEs between MutT and AMPCPP and dGTP protons also indicate substrate binding in this region.

MATERIALS AND METHODS

Materials

The MutT protein and ^{15}N-labeled MutT protein were isolated and purified as previously described (Abeygunawardana *et al.*, 1993; Frick *et al.*, 1994b). The 8-bromo derivatives of ATP and dGTP were synthesized as described (Bhatnagar *et al.*, 1991). AMPCPP was purchased from Sigma, Tris-d_{11} and ^2H_2O were from C/D/N Isotopes. All buffer and nucleotide solutions were passed through a column containing Chelex-100 resin (Bio-Rad) to remove trace metals.

Methods

Enzyme Assays. NTPase assays were performed by measuring pyrophosphate released as previously described (Bhatnagar *et al.*, 1991) at 23 °C in 50 mM Tris-Cl with 8 mM free $MgCl_2$. In a coupled assay, inorganic pyrophosphate was converted to orthophosphate by the presence of 0.5—1.0 units of inorganic pyrophosphatase (EC 3.6.1.1) in the reaction mixture. Reactions were terminated with the addition of one volume of a 4/1 mixture of Norit (20% packed volume)/7% perchloric acid, and nucleotides were removed by centrifugation. Inorganic phosphate was determined in the supernatant using the method of Ames and Dubin (1960). Allowing the pyrophosphate to accumulate and subsequent treatment with pyrophosphatase did not alter the rate. For dGTP, initial velocities were measured at six Mg^{2+}-dGTP concentrations ranging from 0.1 to 2.0 mM. For 8-Br-dGTP, initial velocities were measured at six Mg^{2+}-8-Br-dGTP concentrations ranging from 0.0125 to 0.25 mM. For ATP, initial velocities were measured at six Mg^{2+}-ATP concentrations ranging from 0.1 to 2.0 mM. For 8-Br-ATP, initial velocities were measured at six Mg^{2+}-8-Br-ATP

concentrations ranging from 0.08 to 1.2 mM. K_M and k_{cat} values were obtained by nonlinear regression weighted to substrate concentrations with initial estimates obtained by Lineweaver—Burk analyses.

Sample Preparation for NMR Studies. HSQC titrations of MutT with $MgCl_2$ and Mg^{2+}AMPCPP, were done under conditions very similar to those in which the MutT backbone ^1H's, ^{15}N's, and ^{13}C's were assigned (Abeygunawardana *et al.*, 1993). Samples contained 1.5 mM ^{15}N-labeled MutT, 0.34 mM NaN_3, 0.1 mM EDTA, 6 mM d_{11}-Tris-Cl, pH 7.5, 20 mM NaCl, and 10% ^2H_2O for field-frequency locking. These samples were titrated with $MgCl_2$ from 0 to 2.96 mM and then with Mg^{2+}-AMPCPP from 0 to 6.31 mM, monitoring the ^1H—^{15}N HSQC spectra. For the HSQC titration with Mn^{2+}, a solution containing 0.2 mM ^{15}N-labeled MutT, 5.5 mM AMPCPP, 7.0 mM $MgCl_2$, and the other components listed above was titrated with $MnCl_2$ from 0 to 142 μM. After 2 days at 32 °C MutT retained at least 80% of its activity.

The conformations of bound nucleotides were determined under similar conditions. However, the MutT—Mg^{2+}-AMPCPP—Mg^{2+} complex was found to be unstable at pH 7.5 after 2—4 days but was significantly more stable at slightly higher pH. Therefore, NMR samples used for the determination of the conformation of MutT bound AMPCPP contained, in ^2H_2O, 6 mM d_{11}-Tris-Cl, pH* 8.0 (measured in ^2H_2O, uncorrected for isotope effects), 1.9 mM MutT, 5.3 mM AMPCPP, 13.2 mM $MgCl_2$, 0.34 mM NaN_3, and 0.1 mM EDTA. The enzyme was assayed in NMR samples before and after each NMR experiment as described (Bhatnagar *et al.*, 1991) and was found to retain >95% activity after 7 days at 32 °C.

The NMR samples used to determine the conformation of MutT-bound dGMP contained 2.49 mM MutT, 6.95 mM dGMP, 10.1 mM $MgCl_2$, 47.3 mM NaCl, 0.34 mM NaN_3, 0.1 mM EDTA, 3.64 mM d_{11}-Tris-Cl in ^2H_2O, pH* 8.6. After 5 days at 27 °C the enzyme was 100% active.

^{15}N—^1H Correlation Spectroscopy. All NMR spectra were obtained with a Bruker AM 600 NMR spectrometer. Two-dimensional ^{15}N—^1H HSQC spectra were recorded as previously described (Abeygunawardana *et al.*, 1993). Delay times of 1.5 s and 2.8 ms were used for relaxation and INEPT delays, respectively. A total of 512 t_1 values were recorded using TPPI (Marion & Wüthrich, 1983) with 16 scans per t_1 increment. Acquisition times were 107 (t_1) and 127 ms (t_2). The data were processed with a cosine-bell filter in both dimensions and zero-filled to obtain final matrices of 1K × 1K real data points. The digital resolution was ±0.006 ppm (^1H) and ±0.039 ppm (^{15}N).

^1H—^1H NOESY Spectroscopy. NOESY spectra (Kumar *et al.*, 1980) were acquired in the phase-sensitive mode with use of TPPI (Marion & Wüthrich, 1983). The acquisition parameters were a 1.5 s relaxation delay, a 0.254-s acquisition time, a 8064 Hz sweep width, 4096 time domain data points in F_2, and 1024 time domain data points in F_1. Data sets were collected with mixing times of 200 ms, 100 ms, and twice at 50 ms.

Data were processed both on an Aspect 3000 computer with Bruker software and on a Personal IRIS (Silicon Graphics, Inc.) computer with the program FELIX (Hare, Inc.). All data sets were processed identically with a cosine-bell filter in both dimensions and zero-filling in t_1 to obtain final data matrices of 2K × 2K real data points. After Fourier transformation, the data were phase corrected and

baseline corrected with a second-order polynomial. Fast exchange conditions, suggested by the relatively weak binding of nucleotides to MutT (Frick *et al.*, 1994b), were confirmed by the observation of single NMR spectra for the nucleotides both at 1:1 concentrations and at 3-fold excess of nucleotides over enzyme and by the detection of negative transferred intramolecular NOEs within the nucleotides and negative transferred intermolecular NOEs between MutT and nucleotides at a 3-fold excess of nucleotides.

Sizes of NOE cross peaks were determined, as previously described (Weber *et al.*, 1991). Optimal slices containing the cross peaks were plotted, and the areas were integrated by cutting and weighing the peaks, correcting for scaling factors. Additionally, the sizes of cross peaks were determined by area integration of cross peaks in optimal slices and, for Mg^{2+}-AMPCPP, by volume integration of the cross peaks in 2D NOESY spectra using the program FELIX. No significant differences in interproton distances were obtained by measuring peak areas in optimal slices or peak volumes in 2D NOESY spectra.

Interproton Distance Determinations and Conformational Search Procedures. Distances were initially determined making the two-spin approximation (Rosevear & Mildvan, 1989) leading to an initial set of eight conformations each for Mg^{2+}-AMPCPP and dGMP. These conformations were refined by molecular dynamics (simulated annealing and conjugate gradient minimization) using a full relaxation matrix analysis and back-calculation of the NOESY intensities with the program X-PLOR (Brünger, 1992) in a Convex C220 computer.

In the two-spin approximation, the peak areas and volumes were analyzed using a distance extrapolation method (Beleja *et al.*, 1990) and an initial slope method (Beleja *et al.*, 1990). In the distance extrapolation method, the intensity of each cross peak ($I_{B \to A}$) was compared to the intensity of the reference cross peak between protons at a known distance ($I_{H1' \to H2'}$) for the same mixing time and converted to a distance according to the formula

$$r_{B \to A} = (I_{H1' \to H2'}/I_{B \to A})^{1/6}(r_{H1' \to H2'})$$

where $r_{H1' \to H2'} = 2.90 \pm 0.20$ Å, regardless of the sugar pucker, based on crystal structures of numerous nucleotides (Rosevear & Mildvan, 1989, and references therein). These calculated distances were plotted versus mixing time and extrapolated to zero mixing time by linear least-squares analysis to attenuate the effects of spin diffusion. The use of a reference distance to calculate other distances assumes that the same effective correlation time applies to all interproton interactions. Under fast exchange conditions, as in the present case, the effective correlation time is the concentration weighted average of that of the free and bound nucleotide (Rosevear & Mildvan, 1989, and references therein).

In the initial slope method, the initial slopes of plots of NOE cross peak intensities versus mixing time for proton pairs ($\sigma_{B \to A}$) were compared to the reference initial slope ($\sigma_{H1' \to H2'}$) and converted to distances using

$$r_{B \to A} = (\sigma_{H1' \to H2'}/\sigma_{B \to A})^{1/6}(r_{H1' \to H2'})$$

For the determination of the Mg^{2+}AMPCPP distances, the reference distance from H1' to H2' of 2.90 ± 0.20 Å was

Table 1: Kinetic Parameters of MutT NTPase with Purine Nucleotides

NTP	k_{cat} (s^{-1})	K_m (mM)	k_{cat}/K_m (s^{-1} mM^{-1})	relative k_{cat}/K_m[a]
ATP	0.08 ± 0.006	1.2 ± 0.2	0.067	(1.0)
8-Br-ATP	0.347 ± 0.05	0.64 ± 0.18	0.55	8.2
dGTP	4.0 ± 0.2	0.284 ± 0.05	14.3	(1.0)
8-Br-dGTP	6.6 ± 0.2	0.007 ± 0.001	942	66
8-oxo-dGTP[b]	4.2[b]	0.00048[b]	8750[b]	620

[a] Compared with the corresponding natural nucleotide. [b] From Maki and Sekiguchi (1992).

used, which was the only one available, whereas for the dGMP distances, the more precise reference distance from H1' to H2" of 2.37 ± 0.10 Å was used (Rosevear & Mildvan, 1989), and the distance from H1' to H2' served as a check value.

The initial conformations of Mg^{2+}AMPCPP and dGMP were computed from the measured distances using the program D-SPACE (Hare Research, Inc.). Because no atomic coordinates for AMPCPP were available, they were generated from those of ATP and those of methylene diphosphonic acid (Yount, 1975). In the conformational searches with D-SPACE, the atomic coordinates were randomized by 20 Å movements in all directions, then annealed in four-dimensional space to avoid local minima, and refined by minimizing deviations from all input distances. Over 40 structures of each nucleotide were computed, and, of these, a subset of eight Mg^{2+}-AMPCPP structures and eight dGMP structures were judged acceptable on the basis of consistency with all covalent constraints, angle constraints, van der Waals constraints, and the measured distances within their experimental errors.

These eight structures for each nucleotide then served as input conformations for further refinement by molecular dynamics, i.e., simulated annealing followed by conjugate gradient minimization. In this refinement, the NOEs at each mixing time were analyzed by the complete relaxation matrix with back-calculation of the observed NOESY cross peak intensities. During the refinement, the fit of the interproton distances within each structure to the NOESY data was monitored by a decrease in the generalized R value (James *et al.*, 1991; Nilges *et al.*, 1991) which measures the percent difference between the calculated and observed NOE intensities. The relaxation matrix refinement altered the nucleotide conformations and significantly improved their fit to the input data. For the eight initial structures of Mg^{2+}-AMPCPP, the refinement procedure decreased the average R value from $13.3 \pm 1.7\%$ to $6.5 \pm 1.3\%$. For the eight initial structures of dGMP, refinement decreased the average R value from $7.2 \pm 1.1\%$ to $3.9 \pm 1.2\%$. Further refinement did not significantly improve the R values.

RESULTS

Substrate Preference for C-8-substituted Purine Nucleotides. Table 1 shows the results of a kinetic study of the substrate specificity of the MutT NTPase. The data for 8-oxo-dGTP are from Maki and Sekiguchi (1992) obtained under similar conditions. The MutT enzyme clearly prefers the C-8-substituted derivatives over the corresponding natural NTP's. With guanine nucleotides the presence of a C-8 substitution affects the k_{cat} only slightly (less than 2-fold) but greatly decreases the K_M of MutT for the nucleotide (41−
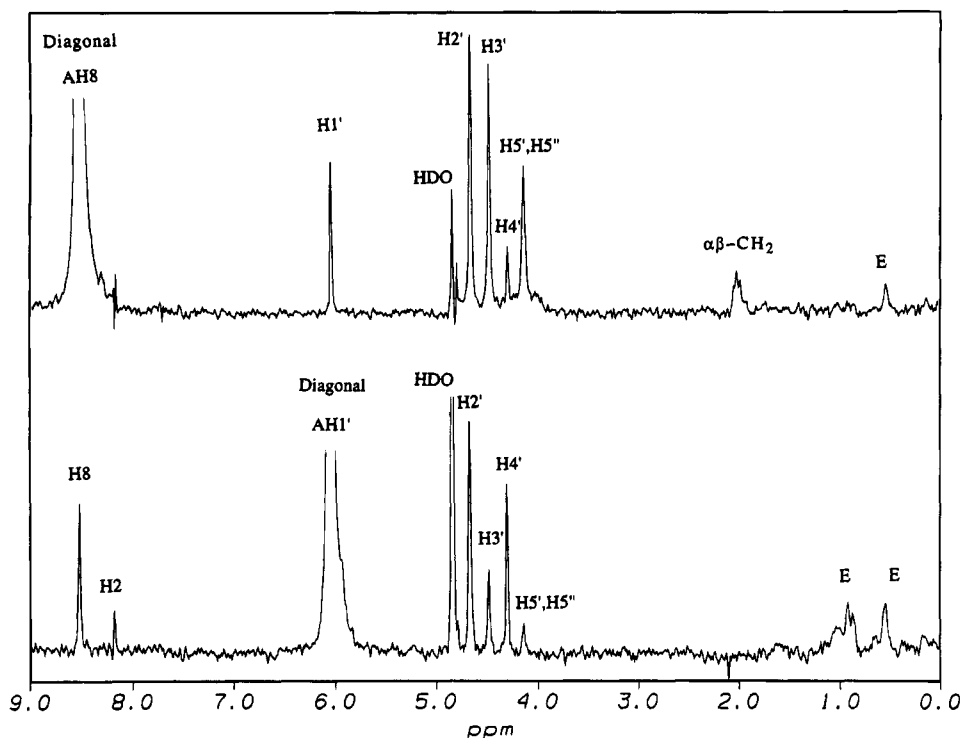
FIGURE 1: Optimal slices from a two-dimensional ^{1}H$-^1$H NOESY spectrum (100 ms mixing time) of MutT-bound Mg^{2+}-AMPCPP. (Upper) Optimal slice (row) through AH8 resonance on diagonal showing negative NOEs to resonances of AMPCPP and MutT, labeled E. (Lower) Optimal slice (row) through AH1' resonance on diagonal showing negative NOEs to resonances of AMPCPP and MutT, labeled E. The sample, in ^{2}H$_2$O, contained 1.9 mM MutT, 5.3 mM AMPCPP, 13.2 mM MgCl$_2$, 0.34 mM NaN$_3$, 0.1 mM EDTA, and 6 mM d$_{11}$-TrisCl, pH* 8.0. $T = 32$ °C.

592-fold). ATP is a poorer substrate for MutT with a k_{cat} 50-fold lower than that of dGTP and a K_M 4.2-fold greater. The 8-bromo substituent on ATP results in a 4.3-fold increase in k_{cat} and a 1.9-fold decrease in K_M (Table 1).

Conformation of Enzyme-Bound Mg^{2+}-AMPCPP. A determination of the conformation of an enzyme-bound purine nucleotide on the MutT enzyme by the nuclear Overhauser effect requires a stable, nonhydrolyzable substrate analog with a proton at position 8. Mg^{2+}-AMPCPP is a linear competitive inhibitor of the MutT enzyme with respect to Mg^{2+}-dGTP with a K_i of 2.4 mM, and dissociation constants of MutT$-$M^{2+}-AMPCPP$-$M^{2+} complexes are similar to the corresponding K_M values for M^{2+}-dGTP (Frick *et al.*, 1994b). Hence AMPCPP was chosen for NMR study. Since adenine nucleotides are not optimal substrates of MutT (Table 1), the conformation of the enzyme-bound product dGMP was also studied for comparison with that of Mg^{2+}-AMPCPP (see below).

The catalytically active form of MutT consists of an enzyme$-$Mg^{2+}-NTP$-$Mg^{2+} complex. Under the conditions of the NMR experiments, it can be calculated from previously measured dissociation constants (Frick *et al.*, 1994b) that more than 99% of the AMPCPP is in the form Mg^{2+}-AMPCPP. The predominant enzyme-bound form (74% of the total enzyme) is in the quaternary MutT$-$Mg^{2+}-AMPCPP$-$Mg^{2+} complex, corresponding to the catalytically active E$-$Mg^{2+}$-$NTP$-$Mg^{2+} species.

Figure 1 (upper) shows an optimal slice (row) from a 2D NOESY spectrum (100 msec mixing time) of the MutT$-$Mg^{2+}$-$AMPCPP$-$Mg^{2+} complex. The resonances of AMPCPP were assigned by comparing the 1D proton NMR spectrum of the nucleotide alone with that of the complex.

The optimal slice through the resonance of adenine H8 on the diagonal (AH8) shows negative NOEs from AH8 to the ribose protons, and to the protons of the α,β-methylene bridge at 2.03 ppm which appears as a pseudotriplet ($^2J_{HP}$ = 16 Hz). The optimal slice through H8 shows qualitatively that the nucleotide is not in a *syn* conformation because H8 gives stronger NOEs to the H2' and H3' protons than to the H1' proton of ribose. The proximity of the H8 to the H5',5" protons is also noteworthy and indicates an *anti* conformation. Figure 1 (lower) shows an optimal slice through the H1' resonance showing negative NOEs from this proton including one to H2' which provides the reference distance.

Table 2 summarizes the initial interproton distances in enzyme-bound Mg^{2+}-AMPCPP obtained with the two-spin approximation and the refined distances obtained by the full relaxation matrix analysis. The former are averages of the distances obtained from four separate data analyses. The peak areas and volumes were each analyzed using both the initial slope and distance extrapolation methods with the reference distance between H1' and H2' of 2.9 $\pm$ 0.2 Å (Rosevear & Mildvan, 1989). The error values take into account uncertainties in peak volume and area measurements, the uncertainty of the reference value, and small, random differences in interproton distances obtained by measuring peak areas or peak volumes. Because of the sixth root relationship between distances and NOE intensities, distance calculations truncate these errors by a factor of 6.

Computation of the relaxation matrix refined distances required an effective correlation time. A value of 2.0 $\pm$ 0.5 ns was calculated from the weighted average of the correlation times of the free nucleotide [0.10 ns (Rosevear *et al.*, 1983)] and the enzyme-bound nucleotide (7.6 ns). The latter value was determined by the Stokes$-$Einstein equation which
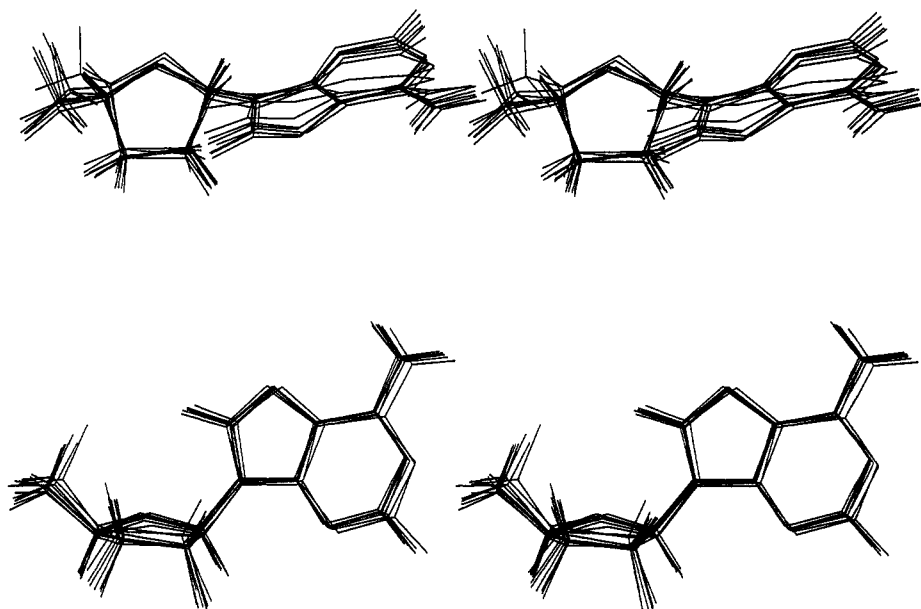
FIGURE 2: Superposition of eight refined conformations of the adenosyl moiety of MutT-bound Mg^{2+}-AMPCPP computed by relaxation matrix analysis and back-calculation of the NOESY intensities using the program X-PLOR (Brünger, 1992). The conformations are refined to R values of 6.5 ± 1.3%, and the RMSD is 0.59 Å. The computed interproton distances and conformational angles are given in Table 2.

Table 2: Interproton Distances Measured for MutT-Bound Mg^{2+}AMPCPP

	distance (Å)	
protons	two-spin approximation[a]	relaxation matrix[b]
AH8 ↔ H1′	3.42 ± 0.20	3.86 ± 0.07
AH8 ↔ H2′	2.78 ± 0.20	2.85 ± 0.10
AH8 ↔ H3′	2.88 ± 0.20	3.05 ± 0.14
AH8 ↔ H4′	3.60 ± 0.45	4.55 ± 0.25
AH8 ↔ H5′,5″	3.32 ± 1.12	3.54 ± 0.52
AH8 ↔ αβCH₂	3.91 ± 1.00	3.97 ± 0.52
AH2 ↔ H1′	4.39 ± 0.20	4.52 ± 0.20
H1′ ↔ H2′	2.90 ± 0.20[c]	2.87 ± 0.10
H1′ ↔ H3′	3.67 ± 0.30	3.95 ± 0.21
H1′ ↔ H4′	3.18 ± 0.22	3.27 ± 0.28
H1′ ↔ H5′,5″	4.83 ± 1.40	4.82 ± 0.60
χ[d]	86 ± 13°	53 ± 9°
δ[e]	131 ± 13°	101 ± 6°

[a]To obtain distances, the peak areas and volumes were analyzed using a distance extrapolation method and an initial slope method (Beleja *et al.*, 1990). In the distance extrapolation method, the intensity of each cross peak ($I_{B→A}$) was compared to the intensity of the reference cross peak ($I_{H1′→H2′}$) and converted to a distance according to the formula $r_{B→A} = (I_{H1′→H2′}/I_{B→A})^{1/6}$ (2.90 Å). These distances were plotted versus mixing time and extrapolated to zero mixing time by linear least squares analysis to correct for spin diffusion. In the initial slope method, the initial slopes of plots of NOE cross peak intensities versus mixing time for proton pairs ($\sigma_{B→A}$) were compared to the reference initial slope ($\sigma_{H1′→H2′}$) and converted to distances using the equation: $r_{B→A} = (\sigma_{H1′→H2′}/\sigma_{B→A})^{1/6}$ (2.90 Å). [b] The procedure is described under Methods. [c] Assumed reference distance (Rosevear & Mildvan, 1989). [d] Mean ± range in eight computed structures of the dihedral angle χ defined by O1′−C1′−N9−C8. [e]Mean ± range in eight computed structures of the dihedral angle δ defined by C5′−C4′−C3′−O3′.

is appropriate for a globular protein like MutT (Abeygunawardana *et al.*, 1995) of molecular weight 14 900. Computed distances were found to be insensitive to variation of the correlation time within its error limits. The validity of the correlation time of 2.0 ± 0.5 ns is indicated by the fact that it yielded the correct reference distance from H1′ to H2′ of 2.87 ± 0.10 Å. The errors in the refined distances (Table 2) reflect the errors in the NOE intensities, and in

the correlation function, truncated by a factor of 6 since a sixth root is taken in the distance calculations.

Full relaxation matrix refinement altered only two of the ten distances calculated with the two-spin approximation, increasing the distances from AH8 to H1′ and to H4′ (Table 2), indicating that these distances are unusually sensitive to spin diffusion. These changes in distance and the refinement procedure, which decreased the R values from 13.3 ± 1.7% to 6.5 ± 1.3%, were sufficient to produce a significant change in the nucleotide conformation. Thus the eight initial structures calculated with the program D-SPACE using the distances obtained with the two-spin approximation showed a high *anti*, C2′-*endo*, O1′-*exo* conformation with $\chi = 86 ± 13°$ and $\delta = 131 ± 13°$.[2] The eight structures refined by the full relaxation matrix analysis to R values of 6.5 ± 1.3% (Figure 2) showed a high-*anti*, C2′-*exo*, O1′-*endo* conformation with $\chi = 53 ± 9°$, $\delta = 101 ± 6°$ and an average RMSD of 0.59 Å (Table 2). The triphosphate chain is not shown in Figure 2 because it is constrained only by the measured distance from AH8 to the α,β-methylene bridge protons.

Conformation of Enzyme-Bound dGMP. Because of the low activity of adenine nucleotide substrates (Table 1), the conformation of enzyme-bound dGMP, a product of the highly active substrate Mg^{2+}-dGTP, was also determined. dGMP binds to the active site of MutT, as shown by the fact that it is a linear competitive inhibitor with respect to Mg^{2+}-dGTP with a K_I of 4.0 ± 1.0 mM (data not shown). Figure 3 shows optimal slices (columns) from a 2D NOESY spectrum (100 ms mixing time) of the enzyme−Mg^{2+}−dGMP complex indicating the assignments of the proton resonances of dGMP. As with enzyme-bound Mg^{2+}-AMPCPP, negative NOEs from GH8 to GH2′ of enzyme-bound dGMP greatly exceed NOEs from GH8 to GH1′ indicating an *anti* conformation (Figure 3, upper). Further, a high-*anti* conformation is indicated by the larger NOE from GH8 to GH2′ than to GH3′ or to GH5′,5″. The weaker

[2] Torsional angles are defined as follows: χ, O4′−C1′−N9−C8; δ, C5′−C4′−C3′−O3′.
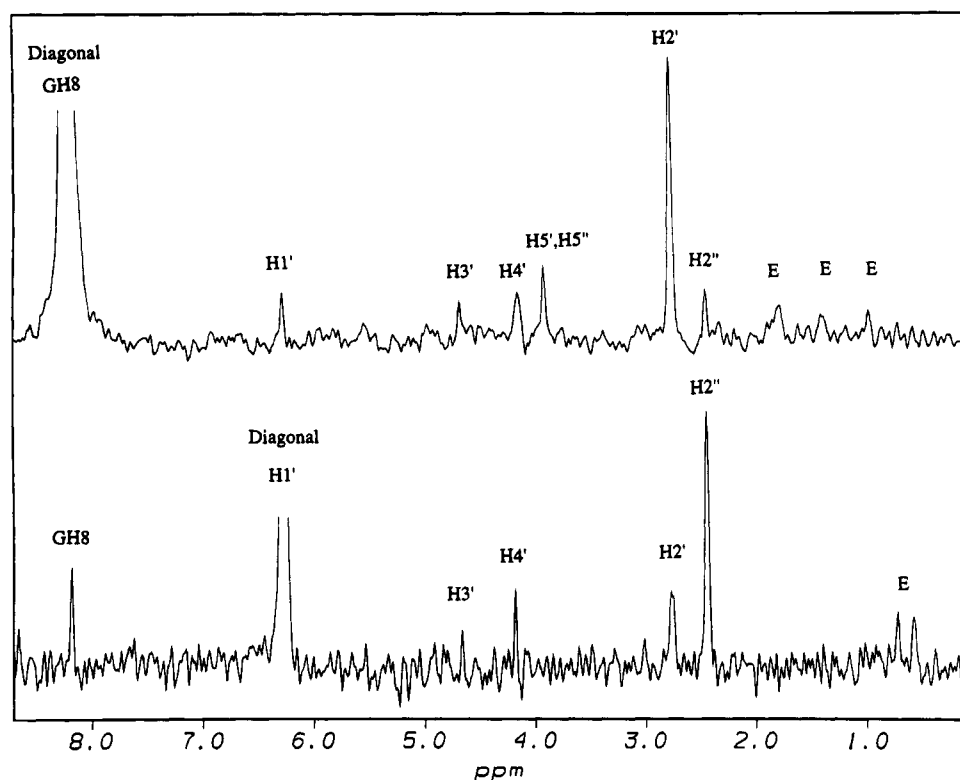
FIGURE 3: Optimal slices from a two-dimensional $^1H-^1H$ NOESY spectrum (100 ms mixing time) of MutT bound dGMP. (Upper) Optimal slice (column) through GH8 resonance on diagonal showing negative NOEs to resonances of dGMP and MutT, labeled E. (Lower) Optimal slice (column) through GH1' resonance on diagonal showing negative NOEs to resonances of dGMP and MutT, labeled E. The sample, in ^2H_2O, contained 2.49 mM MutT, 6.95 mM dGMP, 10.1 mM $MgCl_2$ 47.3 mM NaCl, 0.34 mM NaN_3, 0.1 mM EDTA, and 3.6 mM d_{11}-TrisCl, pH* 8.6. $T = 27$ °C.

NOEs from GH8 to GH3' and to GH5',5'' found with dGMP (Figure 3) than with Mg^{2+}-AMPCPP (Figure 1) result, as shown below, from a different pucker of the deoxyribose ring. The strong cross peak from GH1' to GH2'' (Figure 3, lower) provides a valuable reference NOE at a known interproton distance of 2.37 ± 0.10 Å, regardless of deoxyribose pucker (Rosevear & Mildvan, 1989). As check values, the distances calculated from H1' to H2' with either the two-spin approximation or the full relaxation matrix refinement agree with the known value of 2.90 ± 0.20 Å. The matrix refinement procedure increased the distances from GH8 to H1' and to H2'' indicating these distances to be unusually sensitive to spin diffusion.

The interproton distances in enzyme-bound dGMP agree within error with those found for enzyme-bound Mg^{2+}-AMPCPP with two exceptions, namely, distances from H8 to H2' and from H8 to H3' (Tables 2 and 3). In dGMP H8 is 1.3 ± 0.4 Å closer to H2' than to H3', while in Mg^{2+}-AMPCPP, H8 is, within error, equidistant from H2' and H3'. The eight initial structures calculated with D-SPACE using the distances obtained with the two-spin approximation were high-*anti*, C2'-*endo* ($\chi = 90 \pm 10°$, $\delta = 145 \pm 6°$) while the relaxation matrix refinement, which significantly decreased the R values from 7.2 ± 1.1% to 3.9 ± 1.2% slightly changed the dGMP conformation to high *anti*, C1'-*endo* ($\chi = 73 \pm 9°$, $\delta = 118 \pm 11°$) with an average RMSD of 0.43 Å (Table 3). Figure 4 shows a superposition of the eight refined structures of MutT-bound dGMP. The phosphate is not shown since it is not strongly constrained by the measured distances to H5',5''. The refined conformations of enzyme-bound dGMP and MgAMPCPP are both high-

Table 3: Interproton Distances Measured for MutT-Bound dGMP

protons	distance (Å)	
	2-spin approximation[a]	relaxation matrix[b]
GH8 ↔ H1'	3.44 ± 0.16	3.85 ± 0.14
GH8 ↔ H2'	2.40 ± 0.10	2.33 ± 0.11
GH8 ↔ H2''	3.29 ± 0.10	3.83 ± 0.20
GH8 ↔ H3'	3.83 ± 0.40	3.64 ± 0.28
GH8 ↔ H5',5''	3.73 ± 0.68	3.85 ± 0.57
H1' ↔ H2'	2.89 ± 0.10	2.95 ± 0.17
H1' ↔ H2''	2.37 ± 0.10[c]	2.27 ± 0.07
H1' ↔ H4'	3.26 ± 0.10	3.34 ± 0.08
χ^d	90 ± 10°	73 ± 9°
δ^d	145 ± 6°	118 ± 11°

[a] The methods summarized in Table 2 were used for the determination of the dGMP distances. The more precise reference distance from H1' to H2'' of 2.37 ± 0.10 Å was used (Rosevear & Mildvan, 1989). [b] The procedure is described under Methods. [c] Assumed reference distance. [d] χ and δ are defined in Table 2. Mean ± range in eight computed structures.

anti, with slight differences in the glycosidic torsional angle and in the sugar pucker (Tables 2 and 3; Figures 2 and 4).

Intermolecular NOEs Between MutT and Bound Nucleotides. The NOESY studies also provided intermolecular NOEs from resonances of MutT to those of bound Mg^{2+}-AMPCPP (Figure 1) and to those of bound dGMP (Figure 3) which help to locate the substrate binding site of MutT. Table 4 lists the intermolecular NOEs to the most resolved resonances of the nucleotides seen both in columns and rows at the earliest (50 ms) mixing time. Most were seen at all mixing times. The tentative assignments, based on the
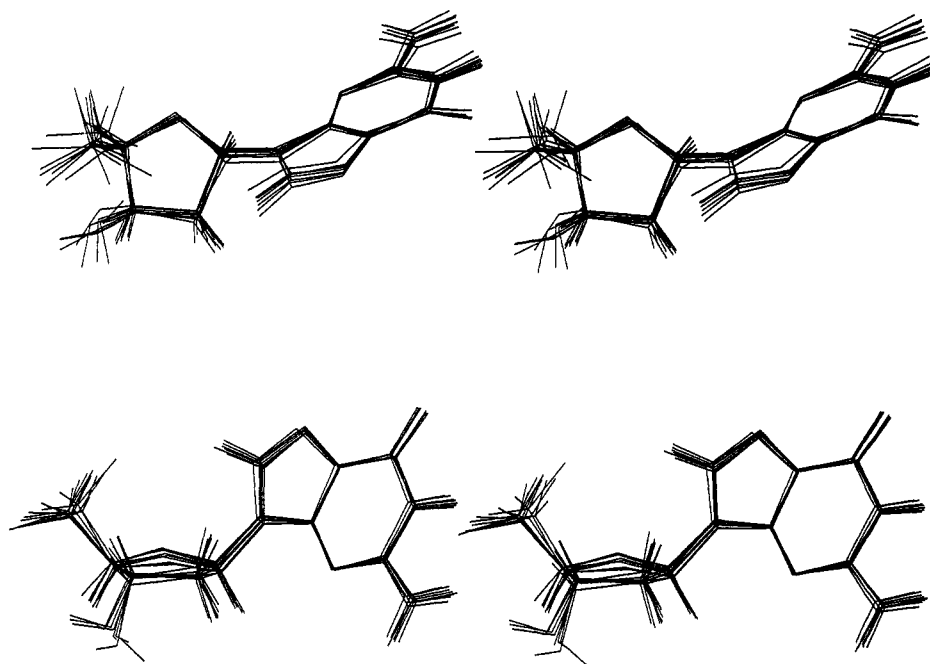
FIGURE 4: Superposition of eight refined conformations of the deoxyguanosyl moiety of MutT-bound dGMP computed by relaxation matrix analysis and back-calculation of the NOESY intensities. The conformations are refined to R values of 3.9 ± 1.2%, and the RMSD is 0.43 Å. The computed interproton distances and conformational angles are given in Table 3.

Table 4: Intermolecular NOEs from the MutT Enzyme to Bound Nucleotides

nucleotide	proton	chemical shift	s/n^a	tentative assignment[c]
AMPCPP	AH8	0.17	2:1	$L67\delta_1$
AMPCPP	AH8	0.55	4:1	$V50\gamma_2$
AMPCPP	AH8	1.74	1.5:1	$L54\gamma_2$ or $L67\beta_2$
AMPCPP	AH2	0.65	6:1	$L54\delta_{1,2}$
AMPCPP	AH2	0.87	4:1	$L67\beta_1, L67\delta_2$
AMPCPP	AH2	1.04	3:1	$L67\gamma$
AMPCPP	AH2	1.19	3:1	$L54\gamma_1$
AMPCPP	AH2	1.75	2:1	$L54\gamma_2$ or $L67\beta_2$
AMPCPP	AH2	7.28	2.5:1	$F68\epsilon$
AMPCPP	AH1'	0.55	4:1	$V50\gamma_2$
AMPCPP	AH1'	0.93	4:1	d
dGMP	GH8	0.59	$3:1^b$	$L54\delta_{1,2}$ or $V50\gamma_2$
dGMP	GH8	1.20	$1.5:1^b$	$L54\gamma_1$
dGMP	GH8	1.41	3:1	$P62\gamma_1$
dGMP	GH8	1.79	2:1	$L54\gamma_2$
dGMP	GH1'	0.60	3:1	$L54\delta_{1,2}$
dGMP	GH1'	0.74	3:1	$V58\gamma_1$
dGMP	GH1'	4.59	$3:1^b$	$V58\alpha$

[a] Signal/noise in optimal slice at 100 ms mixing time. [b] Signal/noise in optimal slice at 50 ms mixing time. [c] Based on chemical shifts in free enzyme and on NOEs to multiple resonances of the same residue. [d] Several possible assignments.

assigned side chain protons of the free enzyme,[3] indicate very similar hydrophobic environments for the purine and sugar moieties of both Mg^{2+}-AMPCPP and dGMP near helix I and loop II of the secondary structure (Figure 5A,B).

HSQC Titrations of MutT with Divalent Cations and AMPCPP. Other clues to the residues involved in metal and substrate binding can be provided by phenomenological effects of Mg^{2+} and Mg^{2+}-AMPCPP on the chemical shifts of the HN and ^{15}N resonances of ^{15}N-labeled MutT. Divalent cations such as Mg^{2+} or Mn^{2+} bind to free MutT at a single site with dissociation constants in agreement with kinetically determined activator constants (Frick *et al.*, 1994b). Figure

[3] C. Abeygunawardana and D. J. Weber, unpublished results, 1994.

5A summarizes the effects of Mg^{2+} (2.96 mM) on the ^1H—^{15}N HSQC spectrum of MutT (1.45 mM) in a titration of the enzyme with $MgCl_2$. On the basis of the previously assigned HSQC spectrum (Abeygunawardana *et al.*, 1993), HN resonances which change in chemical shift by ≥0.05 ppm and ^{15}N resonances which change by ≥0.1 ppm in response to the binding to Mg^{2+} are shown by filled circles on the secondary structure of MutT (Figure 5A). Such changes in chemical shifts of backbone NH and ^{15}N resonances occur at the end of helix I and the beginning of loop II, as well as in loops I and III and in β-strands A and B.

A four-step titration of Mg^{2+}MutT with Mg^{2+}-AMPCPP from 0 to 6.3 mM results in changes in chemical shifts of assigned backbone resonances in the same regions of the enzyme, as indicated by the open circles in Figure 5A. Thus, changes in chemical shift are found at the end of helix I, in loops I and III, and in β-strand A.

Because the changes in chemical shifts reflect indirect as well as direct effects of metal and substrate analog binding, a distance-dependent probe, $MnCl_2$, was titrated into the system. Mn^{2+} is known to occupy both the enzymatic and nucleotide divalent cation binding sites of the E—M^{2+}—AMPCPP—M^{2+} complex with affinities 58- and 71-fold greater, respectively, than Mg^{2+}, and both of these metal binding sites are near each on the triphosphate chain (Frick *et al.*, 1994b). Titration of the enzyme—Mg^{2+}—AMPCPP—Mg^{2+} complex with $MnCl_2$ from 0 to 142 μM resulted in the selective disappearance, due to paramagnetic broadening, of the NH cross peaks of residues G37 (δ 8.14, 109.56 ppm), G38 (δ 8.51, 106.53 ppm), K39 (δ 8.34, 121.80 ppm), and E57 (δ 8.83, 116.45 ppm) indicating proximity of these residues to at least one of the two divalent cation binding sites (data not shown). Thus one or both of the divalent cations, and presumably the triphosphate chain of bound AMPCPP, are near loop I and the end of helix I. Figure 5B summarizes the distance-dependent NMR effects of metal
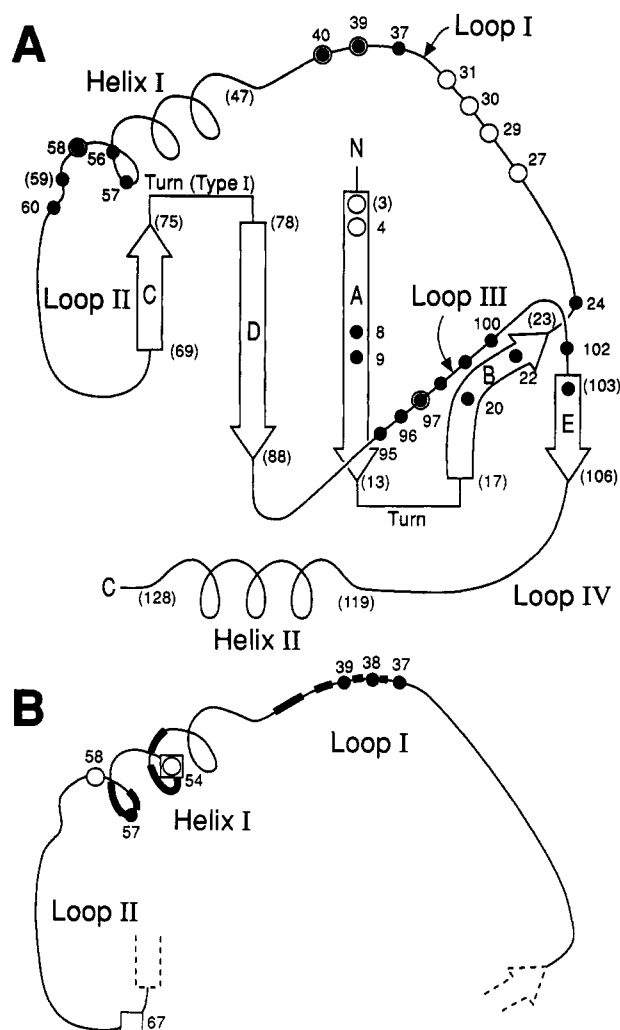
FIGURE 5: Diagram of the secondary structure of MutT (Weber *et al.*, 1993) showing the sites of interaction of divalent cation activators and the substrate analog AMPCPP as detected by NMR. (A) Residues of MutT which show significant changes in chemical shifts of HN (≥ 0.05 ppm) and ^{15}N resonances (≥ 0.1 ppm) in the assigned ^{1}H$-^{15}$N HSQC spectrum of MutT (Abeygunawardana *et al.*, 1993) induced by $MgCl_2$ (●) and by the subsequent addition of Mg^{2+}AMPCPP (○). The numbers in parentheses indicate residues at the beginnings and ends of the secondary structural elements. Experimental conditions are given under Methods. (B) Residues of MutT showing distance dependent effects, i.e., several intermolecular NOEs from AMPCPP (□) and dGMP (○) in NOESY spectra (Table 4). Residues showing disappearance of NH cross peaks in ^{1}H$-^{15}$N HSQC spectra due to paramagnetic broadening by $MnCl_2$ (142 μM) (●) in a system containing 0.2 mM ^{15}N-labeled MutT, 5.5 mM AMPCPP, and 7.0 mM $MgCl_2$. Other components and conditions are given under Methods. The thickened lines show regions of sequence homology among MutT-like pyrophosphohydrolases.

and nucleotide binding and also shows the regions of sequence homology in this group of NTP pyrophosphohydrolases.
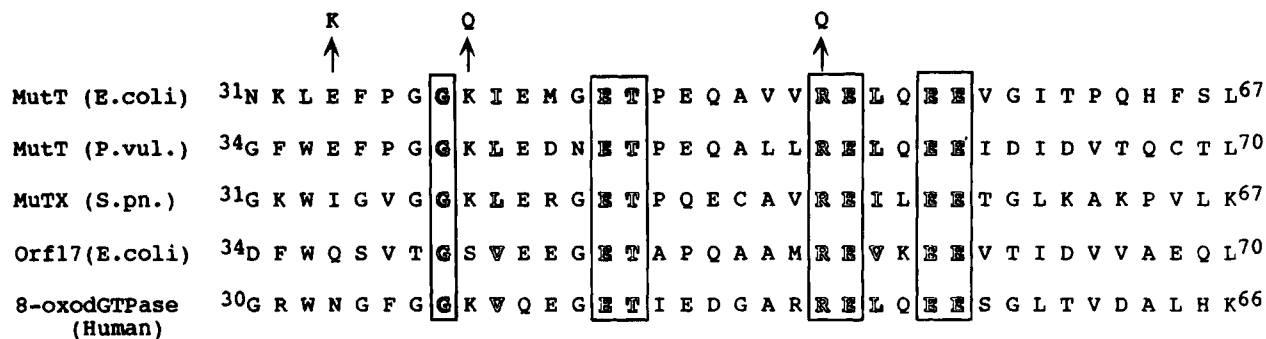
DISCUSSION

To explain the unusual substrate specificity of the MutT enzyme (Table 1), we have examined the conformations of two enzyme-bound nucleotides. Mg^{2+}-AMPCPP was studied since it is a nonhydrolyzable substrate analog that has been shown to be a linear competitive inhibitor with respect to NTP substrates (Frick *et al.*, 1994b). Binding studies revealed quaternary MutT$-$metal$-$AMPCPP$-$metal com-

plexes with dissociation constants similar to those of metal$-$dGTP (Frick *et al.*, 1994b). However, AMPCPP is an analog of ATP which is much less active a substrate than dGTP (Table 1). The 50-fold lower k_{cat} with ATP may reflect an inappropriate nucleotide conformation or interaction with MutT in the active quaternary MutT$-Mg^{2+}-$ATP$-Mg^{2+}$ complex. Because of these possibilities, the conformation of enzyme-bound dGMP, the product of the best natural substrate of MutT, was also studied. Both Mg^{2+}-AMPCPP and dGMP were found to assume high-*anti* conformations on MutT, with similar χ values of $53 \pm 9°$ and $73 \pm 9°$, respectively, supporting the validity of Mg^{2+}-AMPCPP as a substrate analog. While Mg^{2+}-AMPCPP has a C2'-*exo*, O1'-*endo* ribose pucker, dGMP has a C1'-*endo* deoxyribose pucker, a difference which may well reflect the different sugars. The C2'-OH in AMPCPP may force the ribose to assume the C2'-*exo*, O1'-*endo* conformation in order to fit into the MutT active site.

The conformations of MutT-bound nucleotides differ significantly from those found free in solution which are usually mixtures of species. Thus, the conformation of $Co^{3+}(NH_3)_4$ATP in solution is best described as a mixture consisting of 51% high-*anti*, 35% low-*anti*, and 14% *syn* (Rosevear *et al.*, 1983). The conformation of GMP in solution is 53% *syn* and 47% *anti* reflecting the greater tendency of guanine nucleotides to assume *syn* conformations (Son *et al.*, 1972). Binding to MutT simplifies each nucleotide conformation to a single high-*anti* species. Such simplification to a single conformation is generally found with enzymes with high nucleotide specificities (Mildvan, 1989).

The two similar conformations on MutT for two dissimilar nucleotides, Mg^{2+}-AMPCPP and dGMP, indicate that the active site of MutT is specific for a high-*anti* nucleotide conformation. This specificity would permit the MutT enzyme to accommodate nucleotides with bulky substituents at C-8 of the purine ring without intramolecular clashes. An example of such a nucleotide is 8-oxo-dGTP, a preferred substrate for the MutT enzyme (Maki & Sekiguchi, 1992) which can mispair with dA during DNA synthesis with DNA polymerases *in vitro* (Cheng *et al.*, 1991; Maki & Sekiguchi, 1992). The nucleoside 8-oxo-deoxyguanosine prefers the *syn* conformation in solution (Culp *et al.*, 1989) and adopts the *syn* conformation in DNA when mispaired with dA (Kouchakdjian *et al.*, 1991; McAuley-Hecht *et al.*, 1994), thereby avoiding van der Waals overlap with the 5'-CH$_2$ group. A high-*anti* conformation, as found in MutT-bound nucleotides, would also avoid such an intramolecular steric clash in 8-oxo-dGTP (Figures 2 and 4). The architecture of the MutT active site somehow enables the enzyme to discriminate between deleterious and normal nucleotides. The high-*anti* conformations found for Mg^{2+}-AMPCPP and dGMP on MutT are consistent with the suggestion that MutT prevents mispairing during DNA replication by removing mutagenic nucleotides that can readily adopt a *syn* conformation during DNA replication (Maki & Sekiguchi, 1992; Bullions *et al.*, 1994).

Another possible role for the high *anti* conformation of MutT-bound nucleotides is that this conformation might be required for the unusual substitution at the β-phosphorus catalyzed by MutT. Interestingly, phosphoribosyl pyrophosphate synthetase, which also catalyzes nucleophilic substitution at the β-phosphorus of ATP, holds its substrate with a

```
                   K                Q                        Q
                   ↑                ↑                        ↑

MutT (E.coli)   31N K L E F P G G K I E M G E T P E Q A V V R B L Q B B V G I T P Q H F S L67

MutT (P.vul.)   34G F W E F P G G K L E D N B T P E Q A L L R B L Q B B I D I D V T Q C T L70

MuTX (S.pn.)    31G K W I G V G G K L E R G B T P Q E C A V R B I L B B T G L K A K P V L K67

Orf17(E.coli)   34D F W Q S V T G S V E E G B T A P Q A A M R B V K B B V T I D V V A E Q L70

8-oxodGTPase    30G R W N G F G G K V Q E G B T I E D G A R R B L Q B B S G L T V D A L H K66
   (Human)
```

FIGURE 6: Sequence homologies among MutT-like NTP pyrophosphohydrolases. The sequences are from the following sources: *E. coli* MutT (Akiyama *et al.*, 1987); *P. vulgaris* MutT (Kamath & Yanofsky, 1993); *S. pneumoniae* MutX (Mejean *et al.*, 1994); *E. coli* orf17 (Bullions *et al.*, 1994); human 8-oxo-dGTPase (Sakumi *et al.*, 1993). The arrows indicate amino acid changes which significantly decrease MutT activity (see text).

glycosidic torsional angle of 62 ± 5° as determined by Mn^{2+}—proton distances (Granot *et al.*, 1980). This χ value overlaps with those found in MutT bound nucleotides.

The interactions of AMPCPP, dGMP, and divalent cations with MutT, as detected by NMR, provide the first biophysical localization of the active site of this enzyme near the loop I-helix I-loop II region of the secondary structure (Figure 5). Thus, Mg^{2+}-AMPCPP and dGMP both show NOEs to hydrophobic residues of MutT with identical or very similar chemical shifts, indicating proximity (≤ 5 Å) to these residues. Three intermolecular NOEs between Mg^{2+}-AMPCPP and MutT and four intermolecular NOEs between dGMP and MutT can be assigned to the side chain of L54 in helix I. Mg^{2+}-AMPCPP shows three NOEs to the side chain of L67 in loop II and dGMP shows two NOEs to V58 in helix I. Hence, both nucleotides bind at the same or overlapping sites of MutT, supporting the validity of Mg^{2+}-AMPCPP as a substrate analog. It is noteworthy that L54 is conserved either as leucine, isoleucine, or valine in all MutT-like pyrophosphohydrolases (Figure 6). Changes in chemical shifts of backbone ^1H and ^{15}N resonances induced by Mg^{2+} and/or AMPCPP implicate residues in loop I and at the end of helix I, loop III, and β-strands A and B. Mn^{2+}, a distance-dependent paramagnetic probe broadens NH resonances of G37, G38, and K39 in loop I and E57 in helix I. From this we can conclude that these residues are near at least one of the two required metal ions, both of which interact with the triphosphate chain (Frick *et al.*, 1994b). Two of these amino acids, G38 and E57, are conserved in all MutT-like pyrophosphohydrolases (Figure 6).

A role for the loop I—helix I—loop II region of MutT in metal and substrate binding suggested by distance-dependent Overhauser and paramagnetic relaxation effects (Figure 5B) and by less specific chemical shift changes (Figure 5A) is strongly supported by genetic evidence. Sequence homologies with four other enzymes that have MutT-like catalytic activities are found in this region (Figure 6). These enzymes are MutT proteins from *Proteus vulgaris* (Kamath & Yanofsky, 1993) and *Streptococcus pneumoniae* (Mejean *et al.*, 1994), an *E. coli* protein, Orf17, that possesses an NTP pyrophosphorylase activity with a preference for dATP (Bullions *et al.*, 1994), and a human 8-oxo-dGTPase (Sakumi *et al.*, 1993).

The nitrosoguanidine-induced mutation E34K (mutT61), located in loop I, decreases the dGTPase activity of MutT by at least 10^3-fold (Mejean *et al.*, 1994). Site-directed mutagenesis of basic residues were made in loop I (K39Q)

and in helix I (R52Q) (Frick *et al.*, 1994a). In comparison with the wild-type enzyme (Table 1), the K39Q mutant shows an 8-fold decrease in k_{cat} and a 5.3-fold increase in K_m (dGTP) in the Mg^{2+}-activated dGTPase reaction resulting in a 42-fold overall decrease in k_{cat}/K_m. The mutation of a highly conserved Arg residue in helix I, R52Q, results in the loss of all detectable dGTPase activity reflecting, at least, a 10^3-fold loss of catalytic activity (Frick *et al.*, 1994a).

The nucleotide conformations and proximities obtained in this study will aid in the further analysis of the function of the loop—helix—loop active site motif of MutT. They will also permit docking of Mg^{2+}-AMPCPP and dGMP into the active site of MutT when its tertiary structure has been completed. Such studies are currently under way.

ACKNOWLEDGMENT

REFERENCES

Abeygunawardana, C., Weber, D. J., Frick, D. N., Bessman, M. J., & Mildvan, A. S. (1993) *Biochemistry 32*, 13071−13080.

Abeygunawardana, C., Weber, D. J., Gittis, A. G., Frick, D. N., Miller, A. F., Bessman, M. J., Lin, J., & Mildvan, A. S. (1995) *Abstracts of the ASBMB/DBC-ACS Meeting*, San Francisco, CA, May 21−25, 1995 (in press).

Akiyama, M., Takashi, H., & Sekiguchi, M. (1987) *Mol. Gen. Genet. 206*, 9−16.

Ames, B. N., & Dubin, D. T. (1960) *J. Biol. Chem. 235*, 769−775.

Beleja, J. D., Moult, J., & Sykes, B. D. (1990) *J. Magn. Reson. 87*, 375−384.

Bhatnagar, S. A., & Bessman, M. J. (1988) *J. Biol. Chem. 263*, 8953−8957.

Bhatnagar, S. K., Bullions, L. C., & Bessman, M. J. (1991) *J. Biol. Chem. 266*, 9050−9054.

Brünger, A. T. (1992) *X-PLOR Manual*, version 3.1, Yale University Press, New Haven, CT.

Bullions, L. C., Mejean, V., Claverys, J. P., & Bessman, M. J. (1994) *J. Biol. Chem. 269*, 12339−12344.

Cheng, K. C., Cahill, D. S., Kasai, H., Nishimura, S., & Loeb, L. A. (1991) *J. Biol. Chem. 267*, 166−172.

Culp, S. J., Cho, B. P., Kadlubar, F. F., & Evans, F. E. (1989) *Chem. Res. Toxicol. 2*, 416−422.

Fowler, R. G., Amutan, M. V., & Isbell, R. J. (1992) *Mutat. Res. 284*, 307−319.

Frick, D. N., Bullions, L. C., Townsend, B. D., & Bessman, M. J. (1994a) *FASEB J. 8*, A1278.

Frick, D. N., Weber, D. J., Gillespie, J. R., Bessman, M. J., & Mildvan, A. S. (1994b) *J. Biol. Chem. 269*, 1794−1803.

Granot, J., Gibson, K. J., Switzer, R. L., & Mildvan, A. S. (1980) *J. Biol. Chem. 255*, 10931−10937.

James, T. L., Gochin, M., Kerwood, D. J., Pearlman, D. A., Schmitz, U., & Thomas, P. D. (1991) in *Computational Aspects of the Study of Biological Macromolecules by NMR* (Hoch, J. C., Poulsen, F. M., & Redfield, D., Eds.) NATO ASI Series, Vol. 225, pp 331−347, Plenum Press, New York.

Kamath, A. V., & Yanofsky, C. (1993) *Gene 134*, 99−102.

Koonin, E. V. (1993) *Nucleic Acids Res. 21*, 4847.

Kouchakdjian, M., Bodepudi, V., Shibutani, S., Eisenberg, M., Johnson, F., Grollman, A. P., & Patel, D. J. (1991) *Biochemistry 30*, 1403−1412.

Kumar, A., Wagner, G., Ernst, R. R., & Wüthrich, K. (1980) *Biochem. Biophys. Res. Commun. 96*, 1156−1163.

Maki, H., & Sekiguchi, M. (1992) *Nature 355*, 273−275.

Marion, D., & Wüthrich, K. (1983) *Biochem. Biophys. Res. Commun. 113*, 967−974.

McAuley-Hecht, K. E., Leonard, G. A., Gibson, N. J., Thomson, J. B., Watson, W. P., Hunter, W. N., Brown, T. (1994) *Biochemistry 33*, 10266−10270.

Mejean, V., Salles, C., Bullions, L. C., Bessman, M. J., & Claverys, J.-P. (1994) *Mol. Microbiol. 11*, 323−330.

Mildvan, A. S. (1979) *Adv. Enzymol. Relat. Areas Mol. Biol. 49*, 103−126.

Mildvan, A. S. (1989) *FASEB J. 3*, 1705−1714.

Nilges, M., Habazettl, J., Brünger, A. T., & Holak, T. A. (1991) *J. Mol. Biol. 219*, 499−510.

Rosevear, P. R., & Mildvan, A. S. (1989) *Methods Enzymol. 177*, 333−359.

Rosevear, P. R., Bramson, H. N., O'Brian, C., Kaiser, E. T., & Mildvan, A. S. (1983) *Biochemistry 22*, 3439−3447.

Sakumi, K., Furuichi, M., Tsuzuki, T., Kakuma, T., Kawabata, S., Maki, H., & Sekiguchi, M. (1993) *J. Biol. Chem. 268*, 23524−23530.

Son, T., Guschlbauer, W., & Gueron, M. (1972) *J. Am. Chem. Soc. 94*, 7903−7911.

Tavale, S. S., & Sobell, H. M. (1970) *J. Mol. Biol. 48*, 109−123.

Topal, M. D., & Fresco, J. R. (1976) *Nature 263*, 285−293.

Treffers, H. P., Spinelli, V., & Belser, N. O. (1954) *Proc. Natl. Acad. Sci. U.S.A. 40*, 1064−1071.

Weber, D. J., Mullen, G. P., & Mildvan, A. S. (1991) *Biochemistry 30*, 7425−7437.

Weber, D. J., Bhatnagar, S. K., Bullions, L. C., Bessman, M. J., & Mildvan, A. S. (1992) *J. Biol. Chem. 267*, 16939−16942.

Weber, D. J., Abeygunawardana, C., Bessman, M. J., & Mildvan, A. S. (1993) *Biochemistry 32*, 13082−13088.

Yanofsky, C., Cox, E. C., & Horn, V. (1966) *Genetics 55*, 274−281.

Yount, R. G. (1975) *Adv. Enzymol. Relat. Areas Mol. Biol. 43*, 1−56.